An Analysis of Cloud Drop Growth by Collection: Part I. Double Distributions

EDWIN X BERRY

National Science Foundation, Washington, D. C. 20550

RICHARD L. REINHARDT

Sierra Nevada Corporation, Reno 89505

(Manuscript received 29 January 1974, in revised form 9 April 1974)

ABSTRACT

A new, highly accurate, yet fast method for the numerical solution of the stochastic collection equation is described. Basic size distribution parameters are defined that lay a basis for a parameterized description of stochastic collection. Application is made to double initial distributions. A newly defined mode, here designated "large hydrometeor self-collection", is found to occupy an important position along with autoconversion, accretion and breakup in the generalized description of drop growth by collection.

1. Introduction

Berry's (1967) calculations of cloud droplet growth by collection showed the effects of a variety of collection kernels on a single initial distribution. The calculations of Bartlett (1966) showed that distributions having more larger droplets develop faster than those having fewer larger droplets. Similar effects were noted somewhat more quantitatively by Berry (1968a). However, because of the difficulty in constructing numerical methods sound enough to solve the stochastic collection equation with sufficient accuracy in its more unstable modes, reliable quantitative calculations were not available over a wide range of initial conditions.

Very accurate numerical methods have now been developed (described in Appendix A of this paper) and the growth by collection of a variety of initial droplet distributions has been re-calculated.

In this paper we shall look at the development of two selected double initial distributions and then study separately three basic modes of drop growth by collection. The interpretation of these results leads to the definition of a new concept, "large hydrometeor self-collection," which becomes, along with autoconversion, accretion and breakup, one of the four basic processes in cloud drop development.

The range of validity of the stochastic collection equation used here (as in Berry, 1967) has been adequately discussed elsewhere (see Warshaw, 1967, 1968; Scott, 1967, 1968; Berry, 1967, 1968b; Long, 1971, 1972; Scott, 1972; and especially Gillespie, 1972).

Unless otherwise designated, cgs units are used throughout. A list of symbols is given in Appendix B.

2. The model

The droplet distribution is represented by a density function which is proportional to the number of droplets in each size range over a volume in the cloud. The volume is assumed to be large enough to contain a sufficient number of drops of each size to give a meaningful statistical average. The density function used to describe the distribution is independent of the size of the volume since it is an average over the volume. There is no loss of droplets through the boundary of the volume. Drops that would fall out are conceptually replaced randomly in the volume.

The density function will be characterized by $f\langle x\rangle$[1], where $f\langle x\rangle dx$ is the number of droplets per unit volume (cm^{-3}) in the size interval x to $x+dx$ and x is the mass of a droplet.

3. The primary parameters of the distribution

We begin our description with a definition of some basic parameters of a drop spectrum. There are three primary extensive variables which are defined as integrals of the number density function. These are the number concentration N, the liquid water content L,

[1] The use of angle brackets to distinguish a density function from an analytic function follows Berry (1967).

and the spectral radar reflectivity Z, where

$$N=\int f\langle x\rangle dx, \tag{1}$$

$$L=\int xf\langle x\rangle dx, \tag{2}$$

$$Z=\int x^2 f\langle x\rangle dx. \tag{3}$$

The usual radar reflectivity $Z'=\Sigma nd^6$ is related to Z by

$$Z'=(6/\pi\rho)^2 Z, \tag{4a}$$

or

$$Z(\text{gm}^2\text{ cm}^3)=5.24\times10^{-12}\,Z'(\text{mm}^6\text{ m}^{-3}), \tag{4b}$$

where ρ is the density of water. There are also two intensive variables which are defined as

$$x_f=L/N, \tag{5}$$

$$x_g=Z/L, \tag{6}$$

where x_f is the usual "mean mass" of the *number* density function $f\langle x\rangle$, and x_g the mean mass of the *mass* density function $g\langle x\rangle$, where

$$g\langle x\rangle=xf\langle x\rangle. \tag{7}$$

Thus, x_g bears the same relationship to $g\langle x\rangle$ as x_f does to $f\langle x\rangle$. From the above, it is also apparent that these parameters can be defined in terms of the expectation values of x in the spectrum $f\langle x\rangle$:

$$x_f=\langle x\rangle, \tag{8}$$

$$x_g=\langle x^2\rangle/\langle x\rangle. \tag{9}$$

As a measure of the spread of the distribution, we define the mass parameter x_b as the standard deviation of mass about the mean:

$$x_b^2=N^{-1}\int (x-x_f)^2 f\langle x\rangle dx, \tag{10a}$$

$$=\langle x^2\rangle-\langle x\rangle^2, \tag{10b}$$

$$=x_f x_g-x_f^2. \tag{10c}$$

For convenience we also define r_f, r_g, r_b as the radii of spherical drops having masses x_f, x_g, x_b, respectively:

$$r_f=(\tfrac{3}{4}\pi\rho)^{-\frac{1}{3}}x_f^{\frac{1}{3}}, \tag{11a}$$

$$r_g=(\tfrac{3}{4}\pi\rho)^{-\frac{1}{3}}x_g^{\frac{1}{3}}, \tag{11b}$$

$$r_b=(\tfrac{3}{4}\pi\rho)^{-\frac{1}{3}}x_b^{\frac{1}{3}}. \tag{11c}$$

Following Mason (1971) we call x_g the "predominant mass" and r_g the "predominant radius."

A zero superscript will denote values at time zero.

4. The initial distribution

A gamma, or Pearson Type III, distribution, as discussed by Golovin (1963), Berry (1967) and Scott (1968), is used to calculate each initial distribution of cloud droplets. This form, or linear combinations of it, can be used to approximate many measured cloud droplet populations.

The initial density function is

$$f^0\langle x\rangle=Nx_f^{-1}G(\nu)s^\nu e^{-(1+\nu)s}, \tag{12a}$$

where

$$s=x/x_f, \tag{12b}$$

$$G(\nu)=(1+\nu)^{1+\nu}/\Gamma(1+\nu). \tag{12c}$$

The relative variance, var x, of this distribution is

$$\text{var } x=(\langle x^2\rangle-\langle x\rangle^2)/\langle x\rangle^2, \tag{13}$$

$$=1/(1+\nu). \tag{14}$$

As it has been common in microphysical studies to use the relative variance in droplet *radius* rather than in droplet *mass*, a discussion of the difference is warranted.

If $f\langle x\rangle$ is changed to (e.g., Berry, 1967)

$$f\langle r\rangle=(3x/r)f\langle x\rangle, \tag{15}$$

then the relative variance in r may be calculated. There is no easy, direct relationship of var r to var x, but it may be approximated for this initial distribution by

$$\text{var } r\approx 0.14\text{ var } x. \tag{16a}$$

The associated relative dispersions[2] are therefore related by

$$\text{var}^{\frac{1}{2}}r\approx 0.38\text{ var}^{\frac{1}{2}}x. \tag{16b}$$

This approximation and the more accurate relationship are shown in Fig. 1.

From (8), (10b) and (13), we see that

$$x_b=x_f\,\text{var}^{\frac{1}{2}}x. \tag{17}$$

5. The stochastic collection equation

The stochastic collection equation used here is (following Berry, 1967)

$$\partial f\langle x\rangle/\partial t=\int_{x_0}^{x/2} f\langle x-x'\rangle V(x-x'|x)f\langle x'\rangle dx' - \int_{x_0}^{\infty} f\langle x\rangle V(x|x')f\langle x'\rangle dx', \tag{18}$$

where t is time, x_0 the smallest droplet mass for which collection is considered, and $V(x|x')$ the "collection kernel"; V is related to the linear collision efficiency Y_c by

$$V(r|r_s)=\pi r^2 Y_c(r|r_s)^2\Delta v(r,r_s), \tag{19}$$

[2] The relative dispersion in r, i.e., var$^{\frac{1}{2}}r$, was called D by Berry (1968).

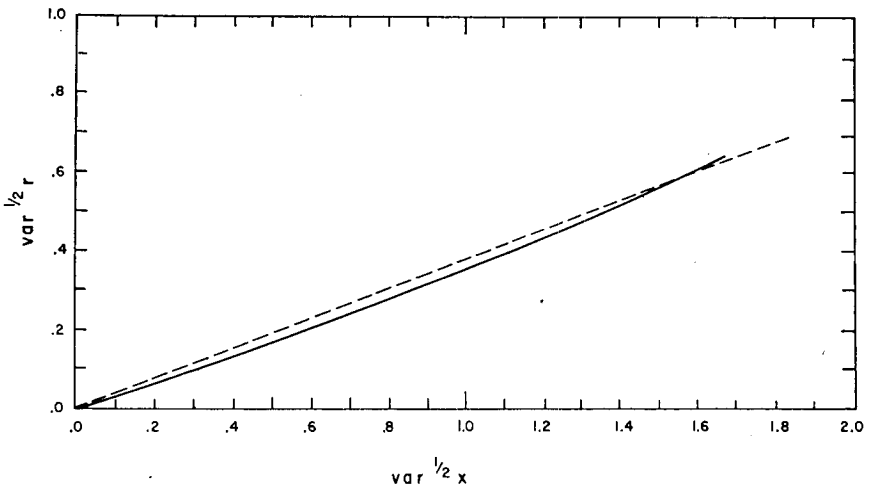

FIG. 1. Relation of the relative dispersion in r to the relative dispersion in x for the gamma-like initial distribution function. Dashed line is $\text{var}^{\frac{1}{2}}r = 0.38\ \text{var}^{\frac{1}{2}}x$.

where r, r_s is the radius of the larger (smaller) droplet, respectively, and Δv the difference in their terminal velocities.

In the calculations reported here the Y_c values of Hocking and Jonas (1970), which agree with those of Davis and Sartor (1967), are used for $r \leqslant 40\ \mu$m and those of Shafrir and Neiburger (1963) are used for $r > 40\ \mu$m. All collisions are assumed to result in a coalescence. Were new information to become available or were it desired to test the effect of electric fields on collection growth, then it would be necessary to rerun the type of calculations described here with a new collection kernel. The parameterizations developed here, however, are given as functions of the collection kernel and would not, therefore, require rederivation from new collection calculations.

Terminal velocities are calculated for an altitude of 1 km by a curve fit to the data of Gunn and Kinzer (1949) according to the method of Berry and Pranger (1974).

All distributions presented have a total of 1 gm m^{-3} of liquid water. The rate of collection, and therefore the rate of change of the distribution, can be shown from (18) to be proportional to the total liquid water.

6. The numerical calculation

A very accurate scheme has been developed for the calculation of particle collection. The method is sufficiently general that it can be applied to a wide variety of problems. A full description is given by Reinhardt (1972) and a summary is given in Appendix A.

While others in the field (e.g., Kovetz and Olund, 1969; Bleck, 1970) have sought faster, approximative methods for solving the collection growth equation, the objectives of this research program have required that accuracy be given first priority and speed the second. In spite of this, the program is not exceptionally time consuming.

By comparison to Bleck's method which takes 11 msec per iteration for a 30-category run on the CDC 6600, our method takes 16 msec. This is not a great difference, particularly when it is noted that we have not especially programmed for speed but have compromised speed for program accuracy and readability. In addition, we have increased the run time over Berry's original method (which took 13 msec for a similar run) as a price for achieving orders of magnitude increase in accuracy.

A misconception that had arisen in some circles to the effect that the method we use consumes excessive computer time stemmed from Thompson's (1968) attempt to find a transformation of the stochastic collection equation that would reduce the computer time consumed for the calculation, on the *assumption* that our method used excessive computer time. This assumption had never been checked, and was the basis for Bleck's claim of having found a "fast" method when the two methods are really of comparable speed.

The accuracy of numerical collection schemes cannot be judged by comparison with the analytic solutions for the constant or sum-of-masses kernel alone, which are the easiest and most fundamental tests of an operating program. Accuracy becomes more difficult to achieve for hydrodynamic kernels and narrow initial density functions. Because of the importance of these latter areas to cloud physics, and because of our suspected numerical spreading error in Berry's original method (although it reproduced the above analytic kernels almost exactly), we have developed a method of calculating collection growth with vastly increased accuracy.

As a part of the work on his dissertation, Reinhardt (1972) tested the accuracy of the numerical formulas used in each step of the calculation. A large variety of formulas were tried and the best ones were selected. So different are the analytic kernels from the real

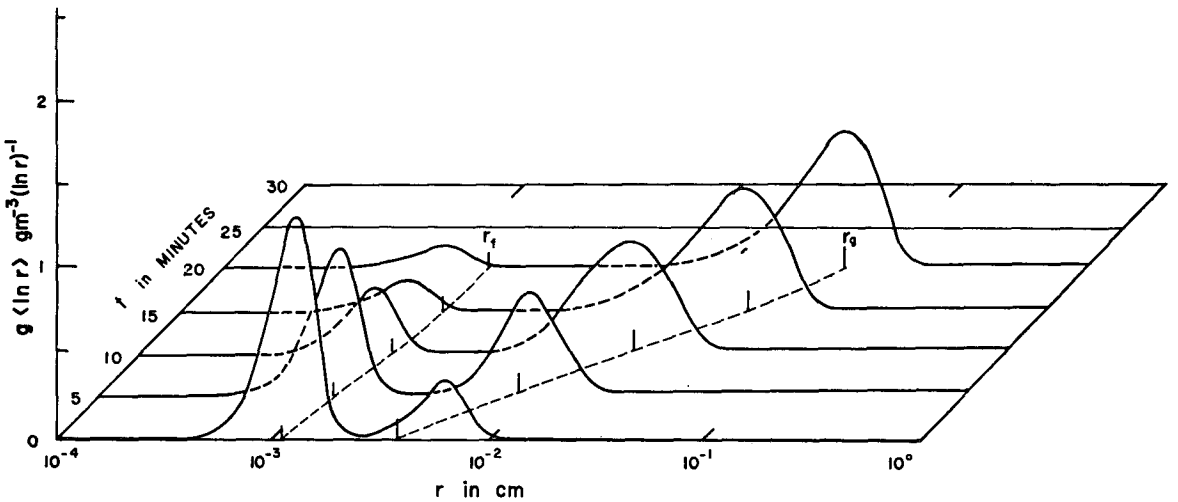

FIG. 2. Time evolution of the initial spectrum composed of 0.8 gm m^{-3} with $r_f^0=10$ μm, and 0.2 gm m^{-3} with $r_f^0=50$ μm, both with var $x=1$.

kernels (which go to zero for like-sized droplets) that the numerical integration formulas giving the best results for the analytic kernels were not the same as the ones giving the best results for the hydrodynamic kernel. Both the interpolating scheme (for finding function values between data points) and the integrating scheme (for evaluating the collection integrals) had to be improved.

The interpolating scheme was tested against analytic values generated from an initial spectrum. The formula selected is a six-point Lagrange interpolation using the natural logarithms of the values to be interpolated. This formula gives four to five place accuracy over the entire range of the spectrum whereas the original method gave one to three place accuracy over the middle of the range but was five orders of magnitude high at the tail.

The integration scheme was checked against devised analytic equations which roughly approximated the integrands found in actual practice. A method giving 100% accuracy was found to be a combination of three- and four-point Lagrangian formulas. When the number of points in the range of integration is odd, the three-point formula is used throughout; when even, the four-point is used at one end, and the three-point is used for the remaining points.

Calculation of the tail is extremely important in obtaining accurate solutions for many realistic cases. The method chosen for allowing the tail of the spectrum to increase to new numerical categories requires that the value in the new category exceed a specified limit within one time step; otherwise, the new value is left at "zero."

Once these methods are established, it is still desirable to have some measure of the accuracy achieved in each particular calculation. An adequate overall test of minimal accuracy was found to be the unphysical change of total liquid water content, so that this single index alone was sufficient to indicate the accuracy of a calculation. The calculations now achieve a 0.15% change in total water over 1800 iterations for the hydrodynamic kernel and a narrow density function, with no artificial constraints on the total water.

This method of checking accuracy would, of course, not hold for a method based upon an inherent conservation of water similar to the splitting method used by Kovetz and Olund (1969). Our tests have shown, however, that the splitting method introduces unacceptable artificial spreading of the droplet spectrum.

The calculations were performed and plots generated on the NCAR CDC 6600/7600. The time step used was 1.0 sec, and 30 min of real time took 10–15 min of computer time on the 6600 and 2–3 min on the 7600.

7. Growth of double distribution

In order to lay a foundation for a following analysis of the growth of single initial distributions, we discuss here the growth of two double distributions. All plots result from the physically realistic collection kernel described above.

Figs. 2 and 3 show the development of two initial spectra each having 0.8 gm m^{-3} of liquid water centered at $r_f^0=10$ μm for the smaller drops and 0.2 gm m^{-3} of liquid water for the larger drops. Fig. 2 has the larger drop population centered at $r_f^0=50$ μm and Fig. 3 has it at $r_f^0=20$ μm. Each of the four individual spectra is generated by use of (12) with $\nu=0$.

Plotted in these figures is the mass density function $g\langle \ln r\rangle$ (gm m^{-3} per unit ln$r$), where

$$g\langle \ln r\rangle = 3x^2 f\langle x\rangle. \tag{20}$$

Unit ln$r$ is a fixed interval at any position on the absissa and is equal to the distance on the ln scale from 1 to e,

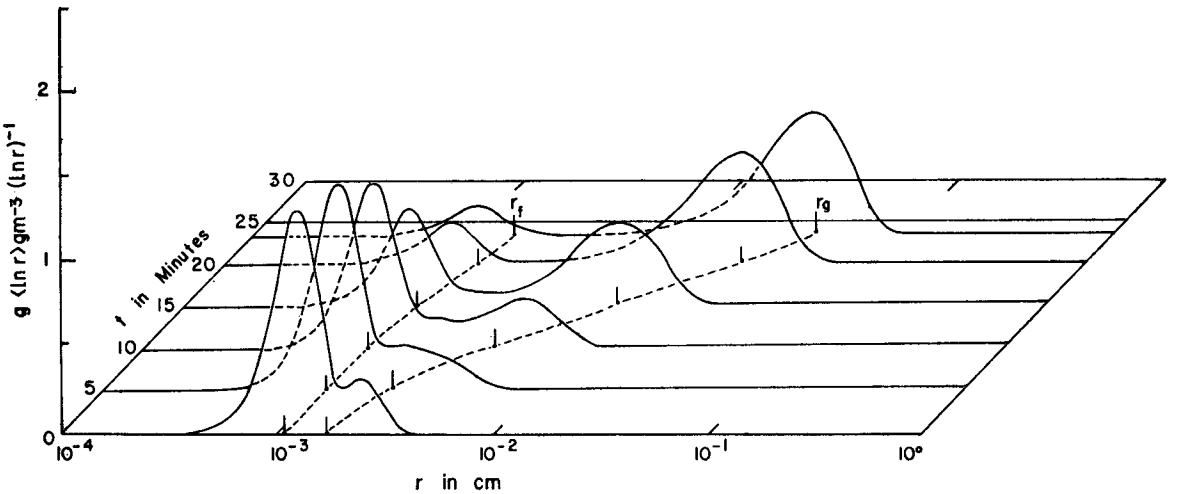

FIG. 3. As in Fig. 2 except for $r_f^0 = 20\ \mu$m.

which is invariant when the radii are multiplied by a constant. Time in minutes is given on the axis projecting inward on the page. Values of r_f and r_g are also plotted against time.

For the purposes of discussion we will break the spectrum of each figure into two parts: we call that on left-hand side "Spectrum one" (or S1) and that on the right "Spectrum two" (or S2). To clarify the designation of quantities which refer specifically to S1 or S2 we will use subscripts 1 and 2, e.g., L_1 or r_{g2}.

We notice how in each case S1 decreases in size with time but stays in the same place, while S2 increases in size as it moves to the right; r_g follows the peak of S2 (at least after S2 has accumulated a sufficient portion of the water), while r_f stays closer to S1. We notice from Eq. (10) that the difference between r_g and r_f is one measure of the spread of the spectrum. Of course, in these two cases r_f is always completely negligible, so from (10c),

$$x_b^2 \approx x_f x_g. \tag{21}$$

By comparing the r_g's and the liquid water on S2 we see that the growth benefit achieved by having S2 centered initially at 50 μm (Fig. 2) rather than 20 μm (Fig. 3) is a lead of about 7.5 min in getting $r_g > 100\ \mu$m. Beyond that there is little difference in the eventual growth.

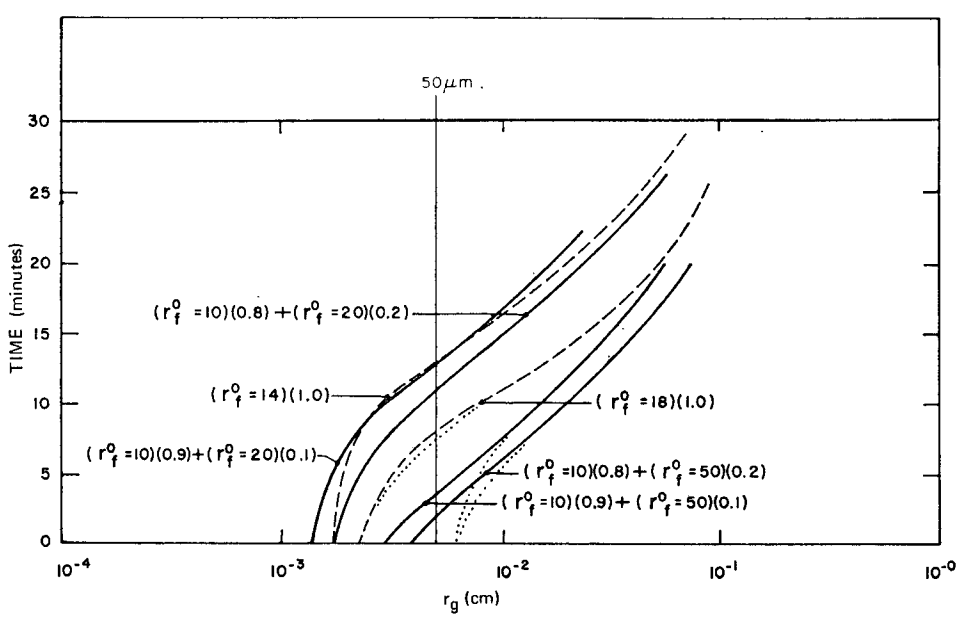

FIG. 4. Time evolution of r_g for four double distributions (solid lines) compared to the single distributions (dashed lines) for $r_f^0 = 14$ and 18 μm. Undesignated values in parentheses are the liquid water contents. The dotted lines show r_{g2}.

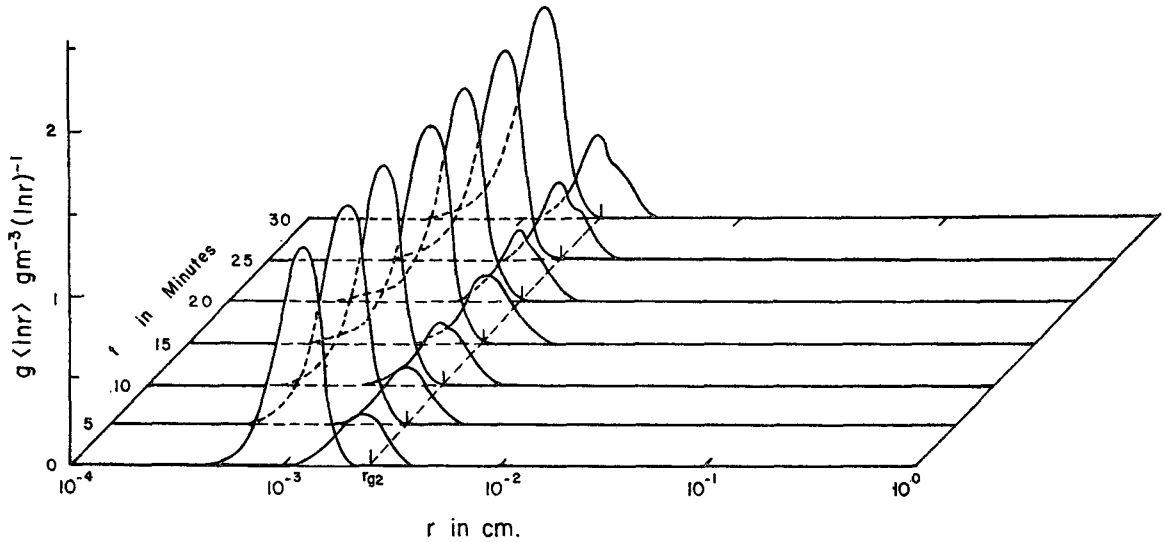

FIG. 5. Time evolution of the initial spectrum given in Fig. 3, with only S1-S1 interactions being allowed.

This comparison of r_g's is shown more precisely in Fig. 4, where we also note the following: (i) the infexion point of most r_g curves occurs between 50 and 100 μm; (ii) the r_g's for $L_2=0.1$ gm m^{-3} lag by only 2 min the corresponding cases of Figs. 2 and 3; (iii) the r_g's (dashed lines) for single initial distributions start slower and then go faster than curves for double distributions; and (iv) the r_g's for larger initial r_{f2} show greater starting rates.

The total growth shown in Figs. 2 and 3 is a composite of three basic modes of interactions. These are the S1-S1 collections (which are referred to as *"autoconversion"*), the S2-S1 collections (which are referred to as *"accretion"*), and the S2-S2 self-collections, a previously undesignated mode that we shall term *"large hydrometeor self-collection."*

Fig. 5 shows the growth due to the S1-S1 self-collections. It is minor in this example. Only a small amount of water is added to S2 and this on the left portion of S2. Since no collection is allowed to occur within S2 no further growth is possible.

Fig. 6 shows the changes due to the S2-S1 collections. This mode also adds water to S2 but the rate of transfer in this case well exceeds that accomplished by the S1-S1 collections of Fig. 5. Judging from this case, accretion is a far more effective mechanism than autoconversion for the transfer of water mass from a small to larger drops. But, although r_{g2} at first moves quite rapidly to the right, it quickly stabilizes as the water transfer becomes more complete. Clearly, a third mechanism is needed to complete the explanation of rapid growth of larger drops.

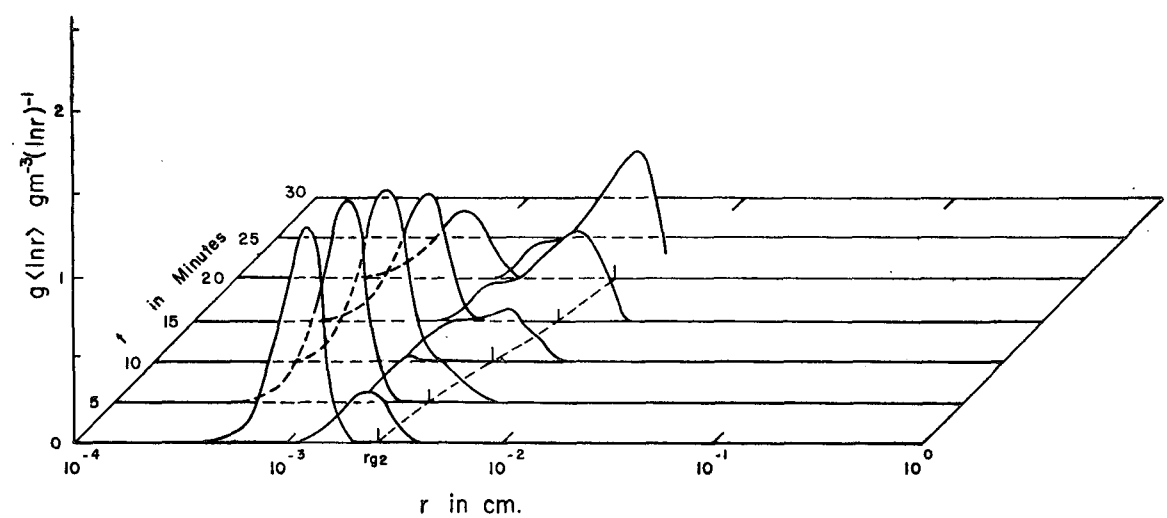

FIG. 6. Time evolution of the initial spectrum given in Fig. 3, with only S2-S1 interactions being allowed.

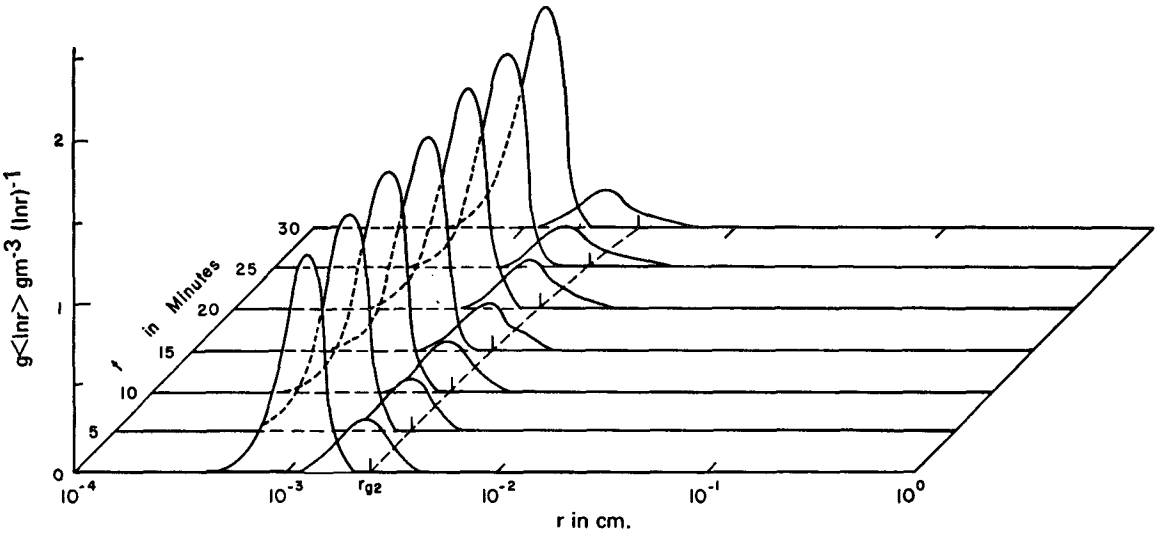

FIG. 7. Time evolution of the initial spectrum given in Fig. 3, with only S2-S2 interactions being allowed.

Fig. 7 shows the action of S2-S2 self-collection alone. It is slow only because L_2 is small. Were $L_2 = 1$ gm m^{-3} the growth by this mode would be five times as fast. The slope does get shallower on the tail and this mode seems to be most responsible for the shallowing of the tail after 5 min in Fig. 3. Were stochastic collection, however, to continue to shallow the tail, then the growth pattern shown in Fig. 3 would not occur.

8. Summary

Three basic modes of collection operate to produce larger drops. The first, autoconversion, serves to add initial water to S2 so that the other modes can operate. It is generally weak by comparison to the other two. The second, accretion, is the primary mechanism for transferring water from S1 to S2. S1 decreases uniformly while keeping its general shape and position as its water mass is transferred to the evolving spectrum S2. Eventually S1 loses almost all of its water to S2. The associated growth produced by this mode on predominant radius of S2 is small, however, as all drops tend to grow at the same rate. (This is similar to graupel growth in a cloud that has an overabundance of ice crystals.)

The third mode, large hydrometeor self-collection, produces large drops quickly. It is responsible for the rapid increase of the predominant radius and the emerging shape of S2. Its rate increases as water mass is added to S2 by accretion. A fourth basic mode, large hydrometeor breakup, will further modify the hydrometeor distribution.

Acknowledgments.[3] The principal author wishes to thank the following for helpful insight, inspiration and guidance to this research: Dr. W. A. Mordy for the research initiation and continued encouragement; Dr. Pierre St.-Amand for the stimulus provided by his many invitations to lecture at the Naval Weapons Center and to participate in the NWC field experiments; Drs. Larry G. Davis and Archie Kahan for the opportunity to participate in conferences and field programs sponsored by the National Science Foundation through Pennsylvania State University, the Sierra Research Corporation, and the Bureau of Reclamation; Drs. F. Winterberg and W. T. Scott for helpful theoretical discussions; Mr. Maarten R. Pranger for improvments to the computer program; and Dr. Dan Gillespie for comments on the manuscript.

The research which provided the basis for this paper was supported by the Atmospheric Sciences Section, National Science Foundation, under Grant GA-21350 to the Desert Research Institute. Numerical calculations were performed on the NSF CDC 6600/7600 at the National Center for Atmospheric Research.

[3] For both Parts I and II.

APPENDIX A

Details of the Collection Calculation

The purpose of this appendix is to present the details of our method for the numerical solution of the stochastic collection equation.[4] The complete program is available upon request.

1. The stochastic collection equation and methodology

The basic physics of collection is contained in the collection kernel V which is defined as the volume swept out per unit time per density of smaller droplets by a larger droplet of radius r within which a collision will occur with a smaller droplet of radius r'. Therefore,

$$V(r|r') = \pi(r+r')^2 \Delta v E, \qquad \text{(A1)}$$

[4] See Reinhardt (1972) for a complete presentation.

where Δv is the difference in terminal fall velocities of the colliding droplets, and E the collision efficiency. In Eq. (A1), which defines the hydrodynamic kernel, two assumptions are made: 1) every collision results in a coalescence; and 2) the viscous forces which inhibit collisions are accounted for by a collision efficiency less than one.

From (A1) it is clear that the probability per unit time that an r droplet will collect an $(r', r'+dr')$ droplet is given by

$$P(r|r')dr' = V(r|r')f\langle r'\rangle dr', \tag{A2}$$

where $f\langle r'\rangle dr'$ is the number of droplets in the range r' to $r'+dr'$.

If x,x' are the masses of the droplets of radius r,r' and some distribution of droplets described by $f\langle x\rangle$ exists at a particular time, the instantaneous rate of change of $f\langle x\rangle$ is given by

$$\frac{\partial f\langle x\rangle}{\partial t} = \int_0^{x/2} f\langle x_c\rangle V(x_c|x')f\langle x'\rangle dx' - \int_0^{\infty} f\langle x\rangle V(x|x')f\langle x'\rangle dx', \tag{A3}$$

where

$$x_c = x - x'. \tag{A4}$$

Eq. (A3) is the stochastic collection equation. It states that $f\langle x\rangle$ is increased by collisions between droplets of mass x_c and x', and that $f\langle x\rangle$ is decreased by collisions between droplets of mass x and x'.

Eq. (A4) is crucial to this method when the continuous spectrum $f\langle x\rangle$ is made discrete so that (A3) can be solved numerically. At that time $f\langle x\rangle$ and $f\langle x'\rangle$ will be known and $f\langle x_c\rangle$ will be found by interpolation.

2. Discretizing the initial distribution and a transformed collection equation

The gamma or Pearson Type III distribution as employed by Scott (1968) is used to specify the initial distribution:

$$f\langle x\rangle = \frac{N^2}{L}\frac{(\nu+1)^{\nu+1}}{\Gamma(\nu+1)}s^{\nu}\exp[-(\nu+1)s], \tag{A5}$$

where N is the total droplet number density (cm^{-3}) L the liquid water content, $s=x/\bar{x}_f{}^0$, $\bar{x}_f{}^0=L/N$, the mean mass of $f\langle x\rangle$, and ν is the width parameter. The relative variance of $f\langle x\rangle$, var x, is $(\nu+1)^{-1}$. The form of this function allows the separate manipulation of L, $\bar{x}_f{}^0$, and var x.

To discretize $f\langle x\rangle$, the following are defined:

$$r(J) = r_0\exp[(J-1)/J_0], \tag{A6}$$

$$x(J) = \tfrac{4}{3}\pi\rho_w r_0{}^3\exp[3(J-1)/J_0]. \tag{A7}$$

In the program $r_0 = 1.968627\times10^{-4}$ cm.

To aid in the solution of (A3), the integrals are evaluated by changing the variable of integration from x' to J'. Thus, the upper limit $x/2$ of the gain integral becomes

$$J_d = J - J_0(\ln 2)/3 = J-2, \tag{A8}$$

thereby defining $J_0 = 6/\ln 2$. From this definition of J_0 and (2.8) and (1.4), the argument of x_c is found to be

$$J_c = J + \frac{2}{\ln 2}\ln[1-2^{(J'-J)/2}]. \tag{A9}$$

For physical and graphical reasons Eq. (A3) is transformed into a mass density per unit $\ln r$, $g\langle\ln r\rangle$. Note that $g\langle q\rangle = xf\langle q\rangle$ where q is a dummy variable. In the program $g\langle\ln r\rangle \equiv G(J)$. For computational purposes a value of G below 10^{-70} gm cm^{-3} per unit $\ln r$ is defined as zero, and the integer argument of the smallest G greater than 10^{-70} is defined as J_m, which now may replace ∞ as the upper limit of the loss integral. In this transformed notation (A3) becomes

$$\frac{\partial G(J)}{\partial t} = \frac{x(J)}{J_0}\left\{\int_1^{J_d} dJ'\frac{x(J)}{x(J_c)}G(J_c)\frac{V(J_c|J')}{x(J_c)x(J')}G(J') - G(J)\int_1^{J_m} dJ'\frac{V(J|J')}{x(J)x(J')}G(J')\right\}. \tag{A10}$$

The $J_0{}^{-1}$ factor is due to changing the variable of integration from $d\ln r$ to dJ. Because g is a density function

$$g\langle\ln r\rangle d\ln r = xf\langle\ln r\rangle d\ln r = xf\langle x\rangle dx, \tag{A11}$$

so that

$$g\langle\ln r\rangle = 3x^2 f\langle x\rangle. \tag{A12}$$

Consequently from (A5) the initial spectrum as used in the program is

$$G(J) = 3L\frac{(\nu+1)^{\nu+1}}{\Gamma(\nu+1)}s^{\nu+2}\exp[-(\nu+1)s], \tag{A13}$$

where $s=x(J)/\bar{x}_{f0}$. As $\bar{x}_f$ is the mean of $f\langle x\rangle$, the number density $\bar{x}_0$ is the mean of $g\langle x\rangle$, the mass density. From (A13) it is found that

$$\bar{x}_{g0} = \left(\frac{\nu+2}{\nu+1}\right)\bar{x}_{f0}. \tag{A14}$$

3. Fall velocity calculation

The terminal velocity of the droplets is calculated from curve fits of Re to $C_d\mathrm{Re}^2$, where Re is the Reynold's number and C_d the drag coefficient. The method is described by Berry and Pranger (1974).

4. Interpolation

Because J_c is not an integer, $G(J_c)$ is not known and must be interpolated. The interpolation method used is a six-point Lagrange interpolation formula. The

following example illustrates how this formula is used:

$$G(J_c)=\exp[A_1\ln G(J-3)+A_2\ln G(J-2)+A_3\ln G(J-1)+A_4\ln G(J)+A_5\ln G(J+1)+A_6\ln G(J+2)], \quad \text{(A15)}$$

where

$$A_1=(-A^5-4A+5A^3)/120, \quad \text{(A16)}$$

$$A_2=[A^4-7A^3+(A^5-A^2+6A)]/24, \quad \text{(A17)}$$

$$A_3=[-A^5+8A^2-12A-(2A^4-7A^3)]/12, \quad \text{(A18)}$$

$$A_4=[3A^4-5A^3+12+(A^5-15A^2+4A)]/12, \quad \text{(A19)}$$

$$A_5=[-A^5+16A^2-(4A^4-A^3-12A)]/24, \quad \text{(A20)}$$

$$A_6=[5A^4-6A+(A^5+5A^3-5A^2)]/120, \quad \text{(A21)}$$

and where

$$A=JC-J=\frac{2}{\ln 2}\ln[1-2^{(J'-J)/2}]. \quad \text{(A22)}$$

This set of coefficients is valid when $J-J'\geqslant 4$. The coefficients are calculated in the polynomial form to eliminate errors that occur when a small number A is subtracted from unity.

When $J-J'=3$, the following set of coefficient is used:

$$A_1=-B/[120(A+4)], \quad \text{(A23)}$$

$$A_2=+B/[24(A+3)], \quad \text{(A24)}$$

$$A_3=-B/[12(A+2)], \quad \text{(A25)}$$

$$A_4=+B/[12(A+1)], \quad \text{(A26)}$$

$$A_5=-B/(24A), \quad \text{(A27)}$$

$$A_6=+B/[120(A-1)], \quad \text{(A28)}$$

where

$$B=(A-1)A(A+1)(A+2)(A+3)(A+4), \quad \text{(A29)}$$

$$A=JC-J. \quad \text{(A30)}$$

These coefficients are employed for interpolation as follows:

$$G(J_c)=\exp[A_1\ln G(J-4)+A_2\ln G(J-3)+A_3\ln G(J-2)+A_4\ln G(J-1)+A_5\ln G(J)+A_6\ln G(J+1)]. \quad \text{(A31)}$$

There are two sets of coefficients because there are two ranges for JC. When $J-J'\geqslant 4$, $J-1<JC<J$, and when $J-J'=3$, $J-2<JC<J-1$. Remember that when $J-J'=2$, $JC=J-2=J'$. The polynomial format is not necessary when $J-J'=3$, because in that case

$$A=JC-J=\frac{2}{\ln 2}\ln(1-2^{-3})=-1.258793747.$$

5. Integration

Over most intervals, three-point Lagrange integration coefficients are used. But, because of the problem presented by the existence of integrands which become zero at certain values of J, special methods are necessary for accurately evaluating the integrals in the neighborhood of the zeros. The zeros occur when like droplets collide ($J=J'$), due to the fact that the collection kernel includes the difference in fall velocities of the droplets. Four- or five-point Lagrange integration coefficients are used in the neighborhood of zero integrands. The following four examples illustrate the integrating technique just described:

a. Even number of points: gain integral: $J_d=8$

$$\int_1^8 \text{aint}\,(J')dJ'=1/3\ \text{aint}\,(1)+4/3\ \text{aint}\,(2)+2/3\ \text{aint}\,(3)+4/3\ \text{aint}\,(4)+1/3\ \text{aint}\,(5)+3/8\ \text{aint}\,(5)+9/8\ \text{aint}\,(6)+9/8\ \text{aint}\,(7)+3/8\ \text{aint}\,(8). \quad \text{(A32)}^4$$

b. Odd number of points: gain integral: $J_d=9$

$$\int_1^9 \text{aint}\,(J')dJ'=1/3\ \text{aint}\,(1)+4/3\ \text{aint}\,(2)+2/3\ \text{aint}\,(3)+4/3\ \text{aint}\,(4)+1/3\ \text{aint}\,(5)+14/45\ \text{aint}\,(5)+64/45\ \text{aint}\,(6)+24/45\ \text{aint}\,(7)+64/45\ \text{aint}\,(8)+14/45\ \text{aint}\,(9). \quad \text{(A33)}^4$$

c. Even number of points through zero integrand: loss integral: $J=8$, $J_m=15$

$$\int_1^{15} \text{aint}\,(J')(dJ')=1/3\ \text{aint}\,(1)+4/3\ \text{aint}\,(2)+2/3\ \text{aint}\,(3)+4/3\ \text{aint}\,(4)+1/3\ \text{aint}\,(5)+3/8\ \text{aint}\,(5)+9/8\ \text{aint}\,(6)+9/8\ \text{aint}\,(7)+3/8\ \text{aint}\,(8)+3/8\ \text{aint}\,(8)+9/8\ \text{aint}\,(9)+9/8\ \text{aint}\,(10)+3/8\ \text{aint}\,(11)+1/3\ \text{aint}\,(11)+4/3\ \text{aint}\,(12)+2/3\ \text{aint}\,(13)+4/3\ \text{aint}\,(14)+1/3\ \text{aint}\,(15). \quad \text{(A34)}^5$$

d. Odd number of points through zero integrand: loss integral: $J=9$, $J_m=16$

$$\int_1^{16} \text{aint}\,(J')dJ=1/3\ \text{aint}\,(1)+4/3\ \text{aint}\,(2)$$

[4] Note that in (A32) and (A33) aint (J') is defined as the appropriate gain integrand and aint $(J_d)=0$.

[5] Note that in (A34) and (A35) aint $(J')=0$ when $J'=J$. Also in the actual calculations J_m is much larger than 16 and aint (J_m) is trivially small so that detailed attention to the integration coefficient at J_m is unnecessary. This fact was meticulously checked.

$$+2/3 \text{ aint } (3)+4/3 \text{ aint } (4)+1/3 \text{ aint } (5)$$

$$+14/45 \text{ aint } (5)+64/45 \text{ aint } (6)+24/45 \text{ aint } (7)$$

$$+64/45 \text{ aint } (8)+14/45 \text{ aint } (9)+3/8 \text{ aint } (9)$$

$$+9/8 \text{ aint } (10)+9/8 \text{ aint } (11)+3/8 \text{ aint } (12)$$

$$+1/3 \text{ aint } (12)+4/3 \text{ aint } (13)+2/3 \text{ aint } (14)$$

$$+4/3 \text{ aint } (15)+1/3 \text{ aint } (16). \quad (A35)^5$$

6. Method of evaluating spectrum growth

The calculation of $\partial G(J)/\partial t$ for $1 \leqslant J \leqslant J_m$ gives the rate of change of the spectrum for existing droplet categories. However, two previously empty, i.e., $G(J)=0$, droplet categories may become occupied after each iteration or time increment. Since $x(J_c)+x(J')=x(J)$ and $x(J+2)=2x(J)$, the two categories, corresponding to J_m+1 and J_m+2, may become occupied by collections between J_c and J' droplets where $J_m-2 \leqslant J_c \leqslant J_m$. If the value of $G(J)$ is greater than 10^{-70} gm cm^{-3} per unit $\ln r$ then the Jth category is occupied by definition. If the value of $G(J)$ is less than 10^{-70} then it is not occupied. This definition results from the finite lower limit of the magnitude of numbers that can be calculated on a computer and facilitates the interpolation as described below.

In calculating $\partial G(J)/\partial t$ for $J=J_m+1$ and $J=J_m+2$, examination of (A10) shows that the loss term is zero since $G(J_m+1)$ and $G(J_m+2)$ are zero. This is physically obvious because non-occupied droplet categories cannot lose droplets. Consequently, only the gain integral need be evaluated for these two cases. This is made clear in the program ("SUBROUTINE SPCHB," where the derivatives are calculated) by the comment "REGION THREE–GAIN ONLY."

The calculation of $G(J_c)$ for these two cases poses a problem because the six-point interpolation scheme uses values of $GL(I)=\ln G(I)$ corresponding to droplet categories where $I>J$ and $\partial G(J)/\partial t$ is to be calculated.

When a spectrum is initialized in the program all values of $G(J)$ less than 10^{-70}, i.e., $J>J_{ni}$, are set equal to zero and the values of GL are set equal to -180, which corresponds to $G=6.0\times10^{-79}$.

Clearly, an accurate interpolation cannot be made when two or more consecutive values of GL are identical as they would be using the six-point scheme for calculating $G(J_c)$ for $J=J_m+1$ and $J=J_m+2$.

This problem is circumvented by using a two-point scheme whenever $GL(J)$ is less than -179. Thus, when $J=J_m+1$ and $J=J_m+2$, $GL(J_c)$ is interpolated using either

$$GL(J_c)=(J_c-J+1)GL(J)+(J-J_c)GL(J-1) \quad (A36)$$

when

$$J-1<J_c<J \quad \text{and} \quad J' \leqslant J-4, \quad (A37)$$

or

$$GL(J_c)=(J_c-J+2)GL(J-1)+(J-J_c-1)GL(J-2) \quad (A38)$$

when

$$J-2<J_c<J-1 \quad \text{and} \quad J'=J-3. \quad (A39)$$

Note that in both cases the coefficients are positive and add to unity.

Once the derivatives $\partial G(J_m+1)/\partial t$ and $\partial G(J_m+2)/\partial t$ are calculated and $G(J_m+1)$ and $G(J_m+2)$ are evaluated, these G values are compared to 10^{-70} gm cm^{-3} per unit $\ln r$. The value of J_m is then increased by one if $G(J_m-1)$ is greater than 10^{-70} and $G(J_m+2)$ is not, or by two if both are greater than 10^{-70}.

7. Modified collection kernel matrix

In (A10) it is seen that V is divided by the product of the masses of the colliding droplets. This form of the equation is used intentionally so that a single matrix W may be used to conserve computer core and to eliminate redundant calculations. Before the actual solution of the equation, $W(J|J')$ is calculated directly and stored in the diagonal and upper right matrix elements, $W(J_c|J')$ is found by interpolating the $W(J|J')$'s and is stored in the lower left matrix elements. When $W(J|J')$ for $J>J'$ is needed in the loss integrand, $W(J'|J)$ is used because V is a symmetric function of its arguments.

8. The computer program

The solutions to the stochastic collection equation presented in this paper were obtained from the following computer program. The intrinsic subroutines called, e.g., ALOG(x) which takes the natural logarithm of x, and the format statements are in the form required by the CDC-6600 or CDC-7600 computers located at the National Center for Atmospheric Research.

The program consists of a main program, six subroutines, and one function subprogram.

The main program performs the following functions:

INITIALIZATION PHASE

1. Reads in the data, which includes:
   a. the value of the smallest radius under consideration R_0;
   b. collision efficiency data called "SARTOR DAVIS KERNEL DATA" in the program;
   c. control parameters.
2. Calculates the radii and masses to be used in the computations.
3. Calculates the terminal fallspeeds of the droplets.
4. Calls subroutine COLPB.
5. Calculates the initial spectrum and its corresponding parameters: N, L, $\bar{x}_f^0$, $\bar{x}_g^0$.
6. Outputs the information obtained in steps 1 through 5, calling subroutine PLOT.

CALCULATION PHASE

1. Calls subroutine SPCHB, which calculates the change in the spectrum due to collections.
2. Calculates resulting spectrum and LWC.
3. Checks for growth of larger droplets, i.e., spectrum spreading.
4. Outputs information obtained in steps 1–3, calling subroutine PLOT.
5. Checks progress of program. The program is terminated if LWC error is above 5% or if time is above maximum time allowed, usually 30 min.
6. If program does not terminate control is returned to 1.

The first subroutine, COLPB, calculates the interpolation and integration coefficients and the modified loss and gain kernels, $W(J,J')=V(J|J')/[x(J)x(J')]$, calculated from the function subprogram V.

The second subroutine, SPCHB, calculates the change in the spectrum, $DG(J)$, and calls subroutines, INTEGL, INTEGG and INTERP, which perform integrations of the loss and gain integrals, and interpolates to find $G(J_c)$, respectively.

The third subroutine, INTEGG, is set up to integrate the gain integral.

The fourth subroutine, INTEGL, is set up to integrate the loss integral.

The fifth subroutine, INTERP, calculates the value of $G(J_c)$ by interpolation.

The sixth subroutine, PLOT, provides the graphical information.

APPENDIX B

List of Symbols

f number density function
g mass density function
L liquid water content
N total number density
r droplet radius
r_b radius corresponding to $x_b=x_f(\text{var } x)^{\frac{1}{3}}$
r_f radius corresponding to $x_f=L/N$
r_g radius corresponding to $x_g=Z/L$
s x/x_f, a parameter used in calculating the initial spectrum
S1 the small hydrometeor or "cloud water" portion of the spectrum
S2 the large hydrometeor portion of the spectrum
V collection kernel
var r relative variance of the spectrum with respect to radius
var x relative variance with respect to mass $[=(x_g/x_f)-1]$
x droplet mass
x_b standard deviation of mass about the mean x_f
x_f mean mass of the number density function
x_g mean mass of the mass density function
Y_c linear collision efficiency
Z spectral radar reflectivity, the second mass moment of the number density function
Z' radar reflectivity $[=(6/\pi\rho)^2Z]$
Δv difference in terminal fallspeeds
ρ density of pure water
ν width of spectrum parameter: var $x=1/(\nu+1)$ for gamma number density function

REFERENCES

Bartlett, J. T, 1966: The growth of cloud droplets by coalescence. *Quart. J. Roy. Meteor. Soc.*, **92**, 93–104.

Berry, E. X, 1967: Cloud droplet growth by collection. *J. Atmos. Sci.*, **24**, 688–701.

——, 1968a: Modification of the warm rain process. *Preprints First Natl. Conf. Weather Modification*, Albany, N. Y., Amer. Meteor. Soc., 81–88.

——, 1968b: Comments on "Cloud droplet coalescence: Statistical foundations and a one-dimensional sedimentation model". *J. Atmos. Sci.*, **25**, 151–152.

——, and M. R. Pranger, 1974: Equations for calculating the terminal velocities of water drops. *J. Appl. Meteor.*, **13**, 108–113.

Bleck, R., 1970: A fast approximative method for integrating the stochastic coalescence equation. *J. Geophys. Res.*, **75**, 5165–5171.

Davis, M. H., and J. D. Sartor, 1967: Theoretical collision efficiencies for small cloud droplets in Stokes flow. *Nature*, **215**, 1371–1372.

Gillespie, D. T., 1972: The stochastic coalescence model for cloud droplet growth. *J. Atmos. Sci.*, **29**, 1496–1510.

Golovin, A. M., 1963: The solution of the coagulating equation for cloud droplets in a rising air current. *Bull. Acad. Sci. USSR, Geophys. Ser.*, No. 5, 482–487.

Gunn, R., and G. D. Kinzer, 1949: The terminal velocity of fall for water droplets in stagnant air. *J. Meteor.*, **6**, 243–248.

Hocking, L. M., and P. R. Jonas, 1970: The collision efficiency of small drops. *Quart. J. Roy. Meteor. Soc.*, **96**, 722–729.

Kovetz, A., and B. Olund, 1969: The effect of coalescence and condensation on rain formation in a cloud of finite vertical extent. *J. Atmos. Sci.*, **26**, 1060–1065.

Long, A. B., 1971: Validity of the finite-difference droplet collection equation. *J. Atmos. Sci.*, **28**, 210–218.

——, 1972: Reply (to Scott). *J. Atmos. Sci.*, **29**, 594–595.

Mason, B. J., 1971: *The Physics of Clouds*. Oxford University Press, pp. 98, 314.

Reinhardt, R. L., 1972: An analysis of improved numerical solutions to the stochastic collection equation for cloud droplets. Ph.D. dissertation, University of Nevada.

Scott, W. T., 1967: Poission statistics in distributions of coalescing droplets. *J. Atmos. Sci.*, **24**, 221–225.

——, 1968: Analytic studies of cloud droplet coalescence 1. *J. Atmos. Sci.*, **25**, 54–65.

——, 1972: Comments on "Validity of the finite-difference droplet collection equation." *J. Atmos. Sci.*, **29**, 593–594.

Shafrir, U., and M. Neiburger, 1963: Collision efficiencies of two spheres falling in a viscous medium. *J. Geophys. Res.*, **68**, 4141–4147.

Thompson, P. D., 1968: A transformation of the stochastic equation for droplet coalescence. *Proc. Intern. Conf. Cloud Phys.*, Toronto, 115–125.

Warshaw, M., 1967: Cloud droplet coalescence: Statistical foundations and a one-dimensional sedimentation model. *J. Atmos. Sci.*, **24**, 278–286.

——, 1968: Cloud-droplet coalescence: Effects of the Davis-Sartor collision efficiency. *J. Atmos. Sci.*, **25**, 874–877.